

Exact scaling functions for one-dimensional stationary KPZ growth

Michael Prähofer and Herbert Spohn,

Zentrum Mathematik and Physik Department, TU München,

D-80290 München, Germany

emails: praehofer@ma.tum.de, spohn@ma.tum.de

With deep appreciation dedicated to Giovanni Jona-Lasinio at
the occasion of his 70th birthday.

Abstract

We determine the stationary two-point correlation function of the one-dimensional KPZ equation through the scaling limit of a solvable microscopic model, the polynuclear growth model. The equivalence to a directed polymer problem with specific boundary conditions allows one to express the corresponding scaling function in terms of the solution to a Riemann-Hilbert problem related to the Painlevé II equation. We solve these equations numerically with very high precision and compare our, up to numerical rounding exact, result with the prediction of Colaiori and Moore [1] obtained from the mode coupling approximation.

1 Introduction

In their well-known work [2] Kardar, Parisi, and Zhang argue that surface growth through random ballistic deposition can be modelled by a stochastic continuum equation, which in the case of a one-dimensional substrate reads

$$\partial_t h = \frac{1}{2} \lambda (\partial_x h)^2 + \nu \partial_x^2 h + \eta. \quad (1.1)$$

Here $h(x, t)$ is the height at time t at location x relative to a suitable reference line. $\eta(x, t)$ is space-time white noise of strength D , $\langle \eta(x, t) \eta(x', t') \rangle = D \delta(x - x') \delta(t - t')$, and models the randomness in deposition. $\nu \partial_x^2 h$ is a not further detailed smoothening mechanism. The important insight of [2] is to observe that the growth velocity is nonlinear, in general, and is relevant for the large scale properties of the solution to (1.1). To simplify, the growth velocity is expanded in the slope. The first two terms can be absorbed through a suitable choice

of coordinate frame. The quadratic nonlinearity in (1.1) is relevant and higher orders can be ignored, unless $\lambda = 0$.

The one-dimensional KPZ equation (1.1) is regarded as exactly solved in the usual terminology. In fact, what can be obtained is the dynamic scaling exponent $z = 3/2$ [3, 2, 4]. No other universal quantity has been computed exactly so far. In our contribution we will improve the situation and explain how to extract the scaling function for the stationary two-point function. A few other universal quantities can be computed as well. But they have been discussed already elsewhere [5, 6, 7].

In [4] a mode-coupling equation for the two-point function is written down, in essence following the scheme from critical dynamics and kinetic theory. At the time only $z = 3/2$ and a few qualitative properties could be extracted from the mode-coupling equation. In [8] this equation is solved numerically. Such computations are repeated in [1] with greatly improved precision and using a more convenient set of coordinates. Thus for the 1D KPZ equation we are in the unique position of an exact solution and an accurate numerical solution to the mode-coupling equation with *no* adjustable parameters. As will be explained below, given the uncontrolled approximation, mode-coupling does surprisingly well.

To attack (1.1) directly does not seem to be feasible, a situation which is rather similar to the one for two-dimensional models in equilibrium statistical mechanics. For example, the Ginzburg-Landau ϕ^4 -theory is given through the (formal) functional measure

$$Z^{-1} \prod_{x \in \mathbb{R}^2} d\phi(x) \exp \left[- \int d^2x \left((\nabla \phi)^2 + g\phi^2 + \phi^4 \right) \right] \quad (1.2)$$

for the scalar field ϕ . (1.2) is not the proper starting point for computing the exact two-point scaling function at the critical coupling g_c . Rather one discretizes through the lattice \mathbb{Z}^2 and replaces the ϕ -field by Ising spins ± 1 . Then, following e.g. [9], the scaling function at and close to criticality can be obtained. By universality this scaling function is the one of (1.2). (While certainly true, to establish universality is difficult and carried out in a few cases only [10].) In the same spirit we replace (1.1) by a discrete model, where the most convenient choice seems to be the polynuclear growth (PNG) model.

Before explaining the PNG model let us review the standard scaling theory for (1.1). If the initial conditions $h(x, 0)$ of the KPZ equation are distributed according to two-sided Brownian motion, then formally the distribution of $h(x, t) - h(0, t)$ is again two-sided Brownian motion. Therefore it is natural to define the stationary time correlation

$$C(x, t) = \langle (h(x, t) - h(0, 0) - t \langle \partial_t h \rangle)^2 \rangle, \quad (1.3)$$

where from the height difference the average displacement is subtracted. By

assumption

$$C(x, 0) = A|x| \quad (1.4)$$

with roughness amplitude $A = D/\nu$ to ensure stationarity in time. If $z = 3/2$, then $C(x, t)$ scales as

$$C(x, t) \propto t^{2/3} g(\text{const} \cdot x/t^{2/3}), \quad \text{as } x, t \rightarrow \infty \quad (1.5)$$

with a universal scaling function $g(y)$ having the asymptotics $g(y) \rightarrow c_0 > 0$ for $y \rightarrow 0$ and $g(y) \sim c_\infty |y|$ for $|y| \rightarrow \infty$. In order to define g as a dimensionless function we fix the proportionality constants in (1.5) as appropriate combinations of λ and A ,

$$g(y) = \lim_{t \rightarrow \infty} \frac{C((2\lambda^2 A t^2)^{1/3} y, t)}{(\frac{1}{2} \lambda A^2 t)^{2/3}}, \quad (1.6)$$

where the particular choice of numerical prefactors is in principle arbitrary. The factor $2^{-2/3}$ in the denominator is chosen in order to conform with the convention for the GUE Tracy-Widom distribution [11]. The factor $2^{1/3}$ in the argument of the numerator differs from the convention used by Baik and Rains [12] by a factor 2 but conforms with the definition of the closely related Airy process [7] and has the further advantage to absorb a lot of prefactors in the equations defining $g(y)$. Note however, that the exponents for the parameters $\lambda[\frac{x^2}{th}]$, $\nu[\frac{x^2}{t}]$, and $D[\frac{h^2 x}{t}]$ are fixed uniquely by dimensional reasoning.

We remark that the slope $\partial_x h(x, t)$ is space-time stationary in the usual sense. For fixed t , $x \mapsto \partial_x h(x, t)$ is white noise with strength A . Since $\langle \partial_x h \rangle = 0$, the standard 2-point function is

$$\langle \partial_x h(0, 0) \partial_x h(x, t) \rangle = \frac{1}{2} \partial_x^2 C(x, t). \quad (1.7)$$

This relation and the asymptotic behavior of g , $g(y)/|y| \rightarrow 2$ as $y \rightarrow \infty$, motivates the definition of a second scaling function,

$$f(y) = \frac{1}{4} g''(y), \quad (1.8)$$

which by definition has integral normalized to one and which will be shown to be positive in the next section.

In the sequel we will analyze the distribution function for the height differences in the stationary PNG model. As shown in [12], they can be represented in terms of certain orthogonal polynomials, which lead to recursion relations connected to the Painlevé II differential equation [13, 14]. The asymptotic analysis is carried out in [12]. Our own contribution is twofold: (i) We observe that the stationary PNG model maps to a last passage percolation with boundaries [6]. (ii) The expressions in [12] are given in terms of certain differential equations and the extraction of the scaling function g requires a careful numerical integration. This is one central point of our article. We will provide then plots of the structure function and give a comparison with the mode-coupling theory.

2 The polynuclear growth model

The polynuclear growth (PNG) model is a model for layer-by-layer growth through deposition from the ambient atmosphere. The surface is parameterized by a time dependent integer-valued height function $h(x, t)$, $t \in \mathbb{R}$, above a one-dimensional substrate, $x \in \mathbb{R}$. Thus the height function consists of terraces bordered by steps of unit height. The up-steps move to the left and the down-steps to the right with speed 1. Steps disappear upon collision. In addition to this deterministic dynamical rule new islands of unit height are nucleated randomly with space-time density 2 on top of already existing terraces. The corresponding stochastic process $h(x, t)$ is well defined even in infinite volume (cf. [15] for the closely related Hammersley particle process).

Of interest to us here is the stationary growth process, which means that the slope $\partial_x h(x, t) = \rho(x, t)$ is stationary in space-time. One can think of $\rho(x, t)$ as the density of a particle/antiparticle process. The particles are located at the up-steps and thus move with velocity -1 , the antiparticles are located at the down-steps and move with velocity 1. Upon collision particle/antiparticle pairs annihilate. In addition, with space-time density 2, a particle/antiparticle pair is created with the particle moving to the left, the antiparticle to the right. To make ρ stationary, one prescribes at $t = 0$ up-steps Poisson distributed with density ρ_+ and down-steps independently Poisson distributed with intensity ρ_- such that

$$\rho_+ \rho_- = 1. \quad (2.1)$$

This measure for steps is stationary under the PNG dynamics. The mean slope is given by

$$u = \rho_+ - \rho_- = \langle \partial_x h(x, t) \rangle, \quad (2.2)$$

which is the only remaining free parameter. For fixed t , $x \mapsto h(x, t) - h(0, t)$ is a (two-sided) random walk with rate ρ_{\pm} for a jump from n to $n \pm 1$. It has average u and variance $\rho_+ + \rho_-$, which implies for the roughness amplitude

$$A(u) = \sqrt{4 + u^2}. \quad (2.3)$$

For the growth velocity one obtains

$$v(u) = \langle \partial_t h \rangle = \rho_+ + \rho_- = \sqrt{4 + u^2}. \quad (2.4)$$

Given $\rho(x, t)$ the height $h(x, t)$ is determined only up to a constant which we fix as $h(0, 0) = 0$. To emphasize that only height differences count, $h(0, 0)$ is sometimes kept in the formulas.

The stationary process with slope u transforms to the stationary process with slope 0 through the Lorentz transformation

$$x' = (1 - c^2)^{-1/2}(x - ct), \quad t' = (1 - c^2)^{-1/2}(t - cx), \quad (2.5)$$

with the speed of “light” equal to 1 and the velocity parameter $c = -u/\sqrt{4+u^2}$. Thus it suffices to restrict ourselves to $u = 0$ which we do from now on. In particular $\rho_+ = 1 = \rho_-$. $\langle \cdot \rangle$ and \mathbb{E} refer to the stationary density field at slope $u = 0$.

The central objects are the height-height correlation

$$C(x, t) = \langle (h(x, t) - h(0, 0) - 2t)^2 \rangle \quad (2.6)$$

and the closely related two-point function for the density,

$$S(x, t) = \langle \rho(x, t) \rho(0, 0) \rangle. \quad (2.7)$$

They are related as

$$\begin{aligned} \frac{1}{2} \partial_x^2 C(x, t) &= \frac{1}{2} \partial_x^2 \mathbb{E} \left((h(x, t) - h(0, 0) - 2t)^2 \right) \\ &= \partial_x \mathbb{E} \left(\rho(x, t) (h(x, t) - h(0, 0) - 2t) \right) \\ &= \partial_x \mathbb{E} \left(\rho(0, t) (h(0, t) - h(-x, 0) - 2t) \right) \\ &= \mathbb{E} (\rho(0, t) \rho(-x, 0)) \\ &= S(x, t). \end{aligned} \quad (2.8)$$

The height correlation is convex, equivalently

$$S(x, t) \geq 0. \quad (2.9)$$

To prove this property we show that the structure function $S(x, t)$ can be regarded as the transition probability for a second class particle starting at the origin. Its initial velocity is ± 1 with probability $\frac{1}{2}$, as for the “first-class” up/down-steps. In contrast to an ordinary step the second class particle is never destroyed upon colliding with another step. Rather it eats up the step encountered and, by reversing its own direction of motion, continues along the trajectory of the absorbed step, cf. Figure 1. Let $\rho(x, t)$ be a given realization of the PNG process. The second class particle is added as

$$\rho^{(\sigma)}(x, 0) = \rho(x, 0) + \sigma \delta(x), \quad \sigma = \pm 1. \quad (2.10)$$

$\rho^{(\sigma)}(x, 0)$ evolves to $\rho^{(\sigma)}(x, t)$ with nucleation events identical to the one for $\rho(x, t)$. By construction, if X_t denotes the position of the second class particle at time t ,

$$\rho^{(\sigma)}(x, t) - \rho(x, t) = \sigma \delta(x - X_t). \quad (2.11)$$

Noting that by the Poisson property $\rho^{(\sigma)}(x, 0)$ is given by $\rho(x, 0)$ conditioned on the presence of either an up-step ($\sigma = +1$) or down-step ($\sigma = -1$) at the origin,

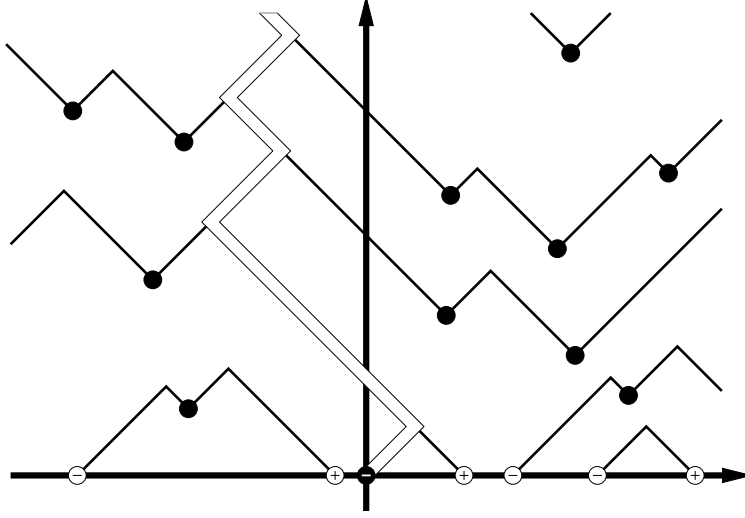


Figure 1: *The trajectory of a second-class particle.*

we obtain

$$\begin{aligned}
0 \leq p_t(x) &= \frac{1}{2} \sum_{\sigma=\pm 1} \mathbb{E} \left(\sigma (\rho^{(\sigma)}(x, t) - \rho(x, t)) \right) = \frac{1}{2} \sum_{\sigma=\pm 1} \mathbb{E} (\sigma \rho^{(\sigma)}(x, t)) \\
&= \lim_{\delta \searrow 0} \frac{1}{2} \sum_{\sigma=\pm 1} \sigma \mathbb{E} \left(\rho(x, t) \middle| \int_{-\delta}^{\delta} \rho(y, 0) dy = \sigma \right) \\
&= \lim_{\delta \searrow 0} \frac{1}{2} \sum_{\sigma, \sigma'=\pm 1} \sigma \sigma' \frac{\mathbb{P} \left\{ \int_{-\delta}^{\delta} \rho(x+y, t) dy = \sigma', \int_{-\delta}^{\delta} \rho(y, 0) dy = \sigma \right\}}{2 \delta \mathbb{P} \left\{ \int_{-\delta}^{\delta} \rho(y, 0) dy = \sigma \right\}} \\
&= \frac{1}{2} \mathbb{E} (\rho(x, t) \rho(0, 0)) = \frac{1}{2} S(x, t).
\end{aligned} \tag{2.12}$$

For arbitrary slope u the normalization of $S(x, t)$ would be given by $v(u) = \sqrt{4 + u^2}$ and the mean of $p_t(x)$ evolves along the characteristics of the macroscopic evolution equation $\partial_t u = -\partial_x v(u)$. Thus

$$\int S(x, t) dx = \sqrt{4 + u^2}, \quad \text{and} \quad \int x S(x, t) dx = -t u. \tag{2.13}$$

3 The distribution functions for the height differences

For the PNG model the distribution function for the height difference $h(x, t) - h(0, 0)$ satisfies certain recursion relations, which are the tool for analyzing the

scaling limit when $t \rightarrow \infty$ and $x = y t^{2/3}$ with $y = \mathcal{O}(1)$. The second moments yield $C(x, t)$ and therefore by (2.8) also $S(x, t)$.

Since the nucleation events are Poisson, $h(x, t) - h(0, 0)$ depends only on the events in the backward light cone $\{(x', t') \in \mathbb{R}^2, 0 \leq t' \leq t, |x - x'| \leq t - t'\}$ and the initial conditions at $t = 0$. Along the line $\{x' = t'\}$ the down-steps are Poisson distributed with line density $\sqrt{2}$ and correspondingly for the up-steps along the line $\{x' = -t'\}$. This property can be deduced from the uniqueness of the stationary state at given slope and the Lorentz invariance (2.5) in the limit $c \rightarrow \pm 1$. Thus $h(x, t) - h(0, 0)$ is determined by the nucleation events in the rectangle $R_{x,t} = \{(x', t') \in \mathbb{R}^2, |x'| \leq |t'|, |x - x'| \leq t - t'\}$ together with the said boundary conditions. $h(x, t) - h(0, 0)$ can be reexpressed as a directed last passage percolation according to the following rules: Inside $R_{x,t}$ there are Poisson points with density 2. Along the two lower edges of $R_{x,t}$ there are independently Poisson points with line density $\sqrt{2}$. A directed passage from $(0, 0)$ to (x, t) is given through a directed path (polymer). It is a piecewise linear path in the plane, starts at $(0, 0)$ and ends at (x, t) , alters its direction only at Poisson points, and is time-like in the sense that for any two points (x', t') , (x'', t'') on the path one has $|x' - x''| \leq |t' - t''|$. Note that, once the directed path leaves one of the lower edges to move into the bulk, it can never return. By definition the length of a directed path equals the number of Poisson points traversed. With these conventions

$$h(x, t) - h(0, 0) = \text{maximal length of a directed path from } (0, 0) \text{ to } (x, t). \quad (3.14)$$

We remark that in general there are several maximizing paths, their number presumably growing exponentially with t .

Under the Lorentz transformation (2.5) the distribution for the height differences (3.14) does not change. Therefore, we might as well transform $R_{(x,t)}$ to a square. By an additional overall scaling by $\sqrt{2}$ one arrives at a $v \times v$ square, $v = \sqrt{t^2 - x^2}$, with bulk density 1 and the line densities $\alpha_- = \alpha = \sqrt{(t-x)(t+x)}$ for the lower left, resp. $\alpha_+ = 1/\alpha$ for the lower right edge. In this way we have recovered precisely the setting in [12, 13] with t replaced by v . Baik and Rains derive an explicit expression for the height distribution in terms of Toeplitz determinants, which can be further simplified by means of corresponding orthogonal polynomials.

Let us state the result for the distribution function of $h(x, t) - h(0, 0)$,

$$\begin{aligned} F_{x,t}(n) &= \mathbb{P}\{h(x, t) - h(0, 0) \leq n\} \\ &= g(n, \alpha)F(n) - g(n-1, \alpha)F(n-1). \end{aligned} \quad (3.15)$$

For fixed v the functions g and F are given in terms of the monic polynomials $\pi_n(z) = z^n + \mathcal{O}(z^{n-1})$, which are pairwise orthogonal on the unit circle $|z| = 1$ with respect to the weight $e^{v(z+z^{-1})}$. Their norm N_n is given by

$$\langle \pi_n, \pi_m \rangle = \delta_{n,m} N_n \quad (3.16)$$

with $\langle p, q \rangle = \oint p(z)q(z^{-1})e^{v(z+z^{-1})}(2\pi iz)^{-1}dz$. One has

$$F(n) = e^{-v^2} \prod_{k=0}^{n-1} N_k, \quad (3.17)$$

where $F(n)$ itself is the distribution function of the maximal length of a directed path in the case $\alpha_+ = 0 = \alpha_-$. Thus $\lim_{n \rightarrow \infty} F(n) = 1$ and

$$\begin{aligned} g(n, \alpha) &= e^{-v(\alpha+\alpha^{-1})} N_n \sum_{k=0}^n N_k^{-1} \pi_k(-\alpha) \pi_k(-\alpha^{-1}) \\ &= e^{-v(\alpha+\alpha^{-1})} \left((1-n) \pi_n(-\alpha) \pi_n(-\alpha^{-1}) \right. \\ &\quad \left. - \alpha \pi_n'(-\alpha) \pi_n(-\alpha^{-1}) - \alpha^{-1} \pi_n(-\alpha) \pi_n'(-\alpha^{-1}) \right). \end{aligned} \quad (3.18)$$

Defining the dual polynomials $\pi_n^*(z) = z^n \pi_n(z^{-1})$, the second equality in (3.18) is an easy consequence of the Christoffel-Darboux formula [16],

$$N_n \sum_{k=0}^{n-1} \frac{\pi_k(a) \pi_k(b)}{N_k} = \frac{\pi_n^*(a) \pi_n^*(b) - \pi_n(a) \pi_n(b)}{1 - ab}, \quad (3.19)$$

valid for $a, b \in \mathbb{C}$, $ab \neq 1$ and extended by l'Hospital's rule to $ab = 1$, and the trivial relation

$$\pi_n^*(z) z^{-1} \pi_n^{*'}(z^{-1}) + z \pi_n'(z) \pi_n(z^{-1}) = n \pi_n(z) \pi_n(z^{-1}) = n \pi_n^*(z) \pi_n^*(z^{-1}). \quad (3.20)$$

Taking only the leading order of a in (3.19) one obtains the well-known relations

$$\begin{aligned} \pi_{n+1}(z) &= z \pi_n(z) + p_{n+1} \pi_n^*(z), \\ \pi_{n+1}^*(z) &= z p_{n+1} \pi_n(z) + \pi_n^*(z), \\ N_{n+1} &= N_n (1 - p_{n+1}^2) \end{aligned} \quad (3.21)$$

which are closed given $p_n = \pi_n(0)$ for $n \geq 0$. For the particular weight function $e^{v(z+z^{-1})}$ one can derive a nonlinear recursion relation for the p_n 's,

$$p_n = -\frac{v}{n} (p_{n+1} + p_{n-1}) (1 - p_n^2), \quad (3.22)$$

with initial values $p_0 = 1$, $p_1 = -\frac{I_1(2v)}{I_0(2v)}$. $I_k(2v) = (2\pi)^{-1} \int_0^{2\pi} e^{ik\theta} e^{2v \cos \theta} d\theta$ is the modified Bessel function of order k and thus $N_0 = I_0(2v)$. Eq. (3.22) is the discrete Painlevé II equation. It has been derived in the context of orthogonal

polynomials for the first time in [14], and later on more or less independently in [17, 18, 13, 19]. The differential equations for π_n , π_n^* ,

$$\begin{aligned}\pi_n'(z) &= (n/z + v/z^2 - p_{n+1}p_nv/z)\pi_n(z) + (p_{n+1}v/z - p_nv/z^2)\pi_n^*(z) \\ \pi_n^{*'}(z) &= (-p_{n+1}v/z + p_nv)\pi_n(z) + (-v + p_{n+1}p_nv/z)\pi_n^*(z),\end{aligned}\quad (3.23)$$

can be shown to hold by a tedious but straightforward induction, using (3.21) and (3.22). We are not aware of any direct reasoning to guess their form. They are implicitly derived in [13], and are written down explicitly here for the first time, to our knowledge.

Of course, the mean of the probability distribution $F_{x,t}(n) - F_{x,t}(n-1)$ is $2t$ and its variance, the correlation function (2.6), is given by

$$C(x, t) = \sum_{n \geq 0} (2(n-2t) - 1) F_{x,t}(n). \quad (3.24)$$

Thus to establish (1.5), one has to understand the scaling properties of the distribution function $F_{x,t}(n)$. Let us introduce the new variables s, y defined by

$$n = 2v + v^{1/3}s, \quad (3.25)$$

$$x = v^{2/3}y, \quad (3.26)$$

where $v = \sqrt{t^2 - x^2}$ is regarded as fixed when varying n and x . In [12] the different scaling variable $w = \frac{1}{2}y$ is used, which leads to a string of factors of 2, avoided by our convention. Setting

$$R_n = -(-1)^n p_n, \quad (3.27)$$

we rewrite (3.22) as

$$R_{n+1} - 2R_n + R_{n-1} = \frac{(\frac{n}{v} - 2)R_n + 2R_n^3}{1 - R_n^2}. \quad (3.28)$$

Under the scaling (3.26), $R_n = v^{-1/3}u(v^{-1/3}(n-2v)) + \mathcal{O}(v^{-1})$, it becomes the Painlevé II equation

$$u''(s) = 2u(s)^3 + su(s), \quad (3.29)$$

in the limit $v \rightarrow \infty$. The starting value $R_0 = -1$ is consistent with the left asymptotics of $u(s)$ only if

$$u(s) \sim -\sqrt{-s/2} \quad \text{as } s \rightarrow -\infty, \quad (3.30)$$

which singles out the Hastings-McLeod solution to (3.29) [20]. This particular solution will be denoted by $u(s)$ and we conclude that

$$u(s) = \lim_{v \rightarrow \infty} v^{1/3} R_{[2v+v^{1/3}s]}, \quad (3.31)$$

provided the limit exists (A complete proof is the main content of [21]). $u(s) < 0$ and u has the right asymptotics

$$u(s) \sim -\text{Ai}(s) \quad \text{as } s \rightarrow \infty. \quad (3.32)$$

At this point we can derive the scaling limit for $F(n)$. It is the GUE Tracy-Widom distribution function [11]

$$F_{\text{GUE}}(s) = e^{-V(s)}, \quad V(s) = - \int_s^\infty v(x) dx, \quad v(s) = (u(s)^2 + s)u(s)^2 - u'(s)^2, \quad (3.33)$$

which appears already as the limiting height distribution for nonstationary curved selfsimilar growth [22]. Since $v'(s) = u(s)^2$, one has $v^{1/3} \log N_{[2v+v^{1/3}s]} \rightarrow v(s)$ and $F([2v+v^{1/3}s]) \rightarrow F_{\text{GUE}}(s)$ as $v \rightarrow \infty$.

Next we turn to the scaling limit for the orthogonal polynomials. For it to be nontrivial we set

$$\begin{aligned} P_n(\alpha) &= e^{-v\alpha} \pi_n^*(-\alpha), \\ Q_n(\alpha) &= -e^{-v\alpha} (-1)^n \pi_n(-\alpha). \end{aligned} \quad (3.34)$$

(3.26) implies $\alpha = 1 - v^{-1/3}y + \mathcal{O}(v^{-2/3})$. Setting n as in (3.25), we claim that

$$a(s, y) = \lim_{v \rightarrow \infty} P_n(\alpha), \quad b(s, y) = \lim_{v \rightarrow \infty} Q_n(\alpha). \quad (3.35)$$

If so, the limit functions a, b satisfy the differential equations

$$\begin{aligned} \partial_s a &= u b, \\ \partial_s b &= u a - y b, \end{aligned} \quad (3.36)$$

as a consequence of (3.21), and

$$\begin{aligned} \partial_y a &= u^2 a - (u' + y u) b, \\ \partial_y b &= (u' - y u) a + (y^2 - s - u^2) b, \end{aligned} \quad (3.37)$$

as a consequence of (3.23). From (3.21) one immediately obtains $\pi_n^*(-1) = (-1)^n \pi_n(-1) = \prod_{k=1}^n (1 - R_k)$. One has the limit $\prod_{k=1}^\infty (1 - R_k) = e^v$ since $e^{-v^2+v} N_0 \prod_{k=1}^n N_k (1 - R_k)^{-1}$ has an interpretation as a probability distribution function [23]. Therefore the initial conditions to (3.37) are

$$a(s, 0) = -b(s, 0) = e^{-U(s)}, \quad U(s) = - \int_s^\infty u(x) dx. \quad (3.38)$$

The scaling limit of $g(n, \alpha)$ as defined in Eq. (3.18) is the function

$$\begin{aligned} g(s, y) &= \int_{-\infty}^s a(s', y) a(s', -y) ds' \\ &= a(s, -y) \partial_y a(s, y) - b(s, -y) \partial_y b(s, y), \end{aligned} \quad (3.39)$$

where the second equality can be verified by differentiation with respect to s and using the identity

$$a(s, y) = -b(s, -y)e^{\frac{1}{3}y^3 - sy}, \quad (3.40)$$

itself being a direct consequence of (3.37) and (3.38). Putting these pieces together we obtain as scaling limit for the distribution functions $F_{x,t}(n)$,

$$F_y(s) = \frac{d}{ds}(g(s + y^2, y)F_{\text{GUE}}(s + y^2)). \quad (3.41)$$

The shift in (3.41) by y^2 comes from the fact that $F_y(s)$ is evaluated for constant $t = v + \frac{1}{2}v^{1/3}y + \mathcal{O}(v^{-1/3})$.

In conclusion we arrive at the scaling function $g(y)$ as defined in the Introduction. From (1.6), with $\lambda = \frac{1}{2}$ and $A = 2$ for the PNG model, and (3.24) we obtain

$$g(y) = \int s^2 dF_y(s). \quad (3.42)$$

As already mentioned, except for (3.23), all our relations are derived in [12, 13], and the existence of limits is proven with Riemann-Hilbert techniques. For completeness let us collect some more properties of a shown in [12]:

$$\begin{aligned} a(s, y) &\rightarrow 1, & \text{as } s \rightarrow +\infty, \\ a(s, y) &\rightarrow 0, & \text{as } s \rightarrow -\infty, \\ a((2y)^{1/2}x + y^2, y) &\rightarrow 1, & \text{as } y \rightarrow +\infty, \\ a((-2y)^{1/2}x + y^2, y) &\rightarrow \frac{1}{(2\pi)^{1/2}} \int_{-\infty}^x e^{-\frac{1}{2}\xi^2} d\xi, & \text{as } y \rightarrow -\infty. \end{aligned} \quad (3.43)$$

Therefore $F_y(s)$ is asymptotically Gaussian and we recover $g(y) \simeq 2|y|$ for large y .

4 Numerical determination of the scaling function

The key object in determining the scaling functions $g(y)$, $f(y)$ is the Hastings-McLeod solution [20] to Painlevé II, $u(s)$, which is the unique solution to

$$u'' = 2u^3 + su \quad (4.1)$$

with asymptotic boundary conditions (3.30) and (3.32). Tracy and Widom [11, 24] integrate (4.1) numerically with conventional differential equation solvers using the known asymptotics at $s = \pm\infty$. The precision achieved with this technique does not suffice for our purposes, since we need $u(s)$ as starting values (3.38) for the differential equations (3.37). We develop here a different method to

obtain $u(s)$, in principle with arbitrary precision. Next the functions $a(s, y)$ and $b(s, y)$ have to be determined, which directly leads to values for the distribution functions $F_y(s)$. They have to be further integrated with respect to s in order to obtain their variance, which is the desired scaling function $g(y)$. The Taylor expansion method to be explained intrinsically produces not only function values at a point but also higher derivatives. Therefore we obtain $f(y)$ not by numerically differentiating $g(y)$ but rather by direct calculation via the knowledge of $\partial_y^2 F_y(s)$.

In a first step, to obtain reliable approximations to the Hastings-McLeod solution, we need a good guess of $u(s)$ at some finite s_0 by using asymptotic expansions around $\pm\infty$. It turns out that the left asymptotics is not well suited to this purpose, since, when integrated along s , the error of an approximation from an optimally truncated asymptotic power series at large negative s always blows up to order 1 near $s = 0$ on an exponential scale. Approximations of the right asymptotics on the other hand allow a, in principle, arbitrary precision on any given finite interval.

For $s \rightarrow \infty$ the deviations of $u(s)$ from the Airy function can be expanded in an alternating asymptotic power series with exponentially small prefactor,

$$u_{\text{right},n}(s) = -\text{Ai}(s) - \frac{e^{-3\zeta}}{32\pi^{3/2}s^{7/4}} \sum_{k=0}^n \frac{(-1)^k a_k}{\zeta^k}, \quad (4.2)$$

with the abbreviation $\zeta = \frac{2}{3}s^{3/2}$. The coefficients are $a_0 = 1$, $a_1 = \frac{23}{24}$, $a_2 = \frac{1493}{1152}$, \dots , and can be obtained via the recursion relation

$$a_n = \text{Ai}_n^{(3)} + \frac{3}{4}n a_{n-1} - \frac{1}{8}(n - \frac{1}{6})(n - \frac{5}{6})a_{n-2} \quad \text{for } n \geq 0 \quad (4.3)$$

with initial conditions $a_{-1} = a_{-2} = 0$.

$$\text{Ai}_n^{(3)} = \sum_{0 \leq k \leq l \leq n} \text{Ai}_{n-l} \text{Ai}_{l-k} \text{Ai}_k. \quad (4.4)$$

are the coefficients in the asymptotic expansion of $\text{Ai}(x)^3$ and

$$\text{Ai}_n = \frac{(6n-1)(6n-5)}{72n} \text{Ai}_{n-1}, \quad \text{Ai}_0 = 1 \quad (4.5)$$

are the coefficients of the asymptotic expansion of the Airy function itself [25],

$$\text{Ai}(s) \sim \frac{e^{-\zeta}}{2\sqrt{\pi}s^{1/4}} \sum_{n \geq 0} \frac{(-1)^n}{\zeta^n} \text{Ai}_n. \quad (4.6)$$

Empirically we observe that for $s_0 \gg 0$ the optimal truncation in (4.2) is $n \approx \frac{4}{3}s_0^{3/2}$ leading to an exponentially improved precision

$$\left| \frac{u_{\text{right},n}(s_0) - u(s_0)}{u(s_0)} \right| \approx \exp(-\frac{8}{3}s_0^{3/2}). \quad (4.7)$$

Linear perturbation around the true solution tells us that the precision of the approximate solution decreases rapidly when integrating in the positive direction, such that $u_{\text{right},n}(s)/u(s) - 1$ is of order one at $s \approx 3^{2/3}s_0 = 2.08s_0$, but the accuracy is still $\approx \exp(-2s_0^{3/2})$. In the negative direction the accuracy decreases but the precision of the approximation stays roughly constant down to $s = 0$. For negative values of s , accuracy and precision are similar, since $u(s)$ is approximately of order 1. Accuracy is lost completely at about $-2s_0$, but at $-2^{1/3}s_0 = -1.26s_0$ still half of the accuracy, $\exp(-1.33s_0^{3/2})$, is retained. What remains is to integrate (4.1) with initial values $u(s_0) = u_{\text{right},n}(s_0)$, $u'(s_0) = u'_{\text{right},n}(s_0)$, $n = [\frac{4}{3}s_0^{3/2}]$.

To solve initial value problems for ordinary differential equations highly sophisticated iteration schemes are available, like Runge-Kutta, Adams-Bashford and multi-step methods. For arbitrary high (but fixed) precision results, all these methods become ineffective, since the step size is a decreasing function of the required precision goal for the solution and tends to become ineffectively small. The only remaining choice is to Taylor expand the solution at a given point. The step size is limited by the radius of convergence only and the precision is controlled by the error made in truncating the Taylor series at some order [26].

$u(s)$ is expanded at s_0 as

$$u(s) = \sum_{n \geq 0} u_n (s - s_0)^n. \quad (4.8)$$

For the Painlevé II equation the expansion coefficients u_n at s_0 are determined by $u_0 = u(s_0)$, $u_1 = u'(s_0)$ and

$$u_{n+2} = \frac{2u_n^{(3)} + s_0 u_n + u_{n-1}}{(n+2)(n+1)}, \quad (4.9)$$

where $u_n^{(k)} = \sum_{j=0}^n u_{n-j} u_j^{(k-1)}$ are the expansion coefficients of $u(s)^k$ at s_0 , $u_n^{(1)} = u_n$. We include the factorial into the expansion coefficients instead of taking the bare Taylor coefficients, in order to reduce the workload from multiplications by binomials when multiplying two expansions numerically.

Numerically we find that the Hastings-McLeod solution does not have any pole in a strip $|\text{Im}(s)| < 2.9$. To have a safety margin we choose a step size one for the extrapolation of the expansion (4.8).

We take the starting values $u(s_0)$, $u'(s_0)$ from (4.2) at $s_0 = 100$. The coefficients of the functions $U(s)$, $V(s)$, see (3.33) and (3.38), when expanded around s_0 are given by

$$U_{n+1} = \frac{u_n}{n+1}, \quad V_{n+2} = \frac{u_n^{(2)}}{(n+2)(n+1)}, \quad n \geq 0, \quad (4.10)$$

and $V_1 = u_0^4 - u_1^2 + s_0 u_0^2$, leaving unspecified the yet unknown integration constants U_0 and V_0 . By means of the recursion relation (4.9) one determines the values of

u , u' , U , and V at $s = s_0 \pm 1$, with these new values at $s = s_0 \pm 2$ and so on. The precision of the integration is in principle only limited by the error in the initial conditions at s_0 . In practice the numerical errors from iterating (4.9) and from truncating (4.8) are easily controlled such that they can be neglected compared to the initial uncertainty. The precision of the approximated values is of order 1 at $s = 200$ (with an accuracy of $\approx 10^{-870}$) and we a posteriori assign to $U(s_0)$ and $V(s_0)$ values, such that $U(200) = V(200) = 0$. The arithmetic computing is done with the C++-based multiprecision package **MPFUN++** [27]. At the end of this first step we have at our disposal the values for u, u', U, V at the integers in the interval $[-20, 200]$. For the convenience of the interested reader let us just state the results at $s = 0$ up to 50 digits,

$$\begin{aligned} u(0) &= -0.367061551548078427747792113175610961512192053613139, \\ u'(0) &= 0.295372105447550054557007047310237988227233798735629, \\ U(0) &= 0.336960697930551393597884426960964843885993886628226, \\ V(0) &= 0.0311059853063123536659591008775670005642241689547838, \end{aligned}$$

which might be used as starting values for a quick conventional integration of Painlevé II to reproduce parts of our results with much less effort but also less precision.

The next step is to determine $a(s, y)$, $b(s, y)$ at $s_0 \in \{-20, \dots, 200\}$ in the interval $y \in [-9, 9]$ employing (3.37) and (3.38). Setting

$$\begin{aligned} a(s, y) &= \sum_{m,n \geq 0} a_{m,n}(s - s_0)^m (y - y_0)^n, \\ b(s, y) &= \sum_{m,n \geq 0} b_{m,n}(s - s_0)^m (y - y_0)^n, \end{aligned} \tag{4.11}$$

(3.37) becomes a recursion relation for the expansion coefficients,

$$\begin{aligned} a_{m,n+1} &= \frac{1}{n+1} \sum_{k=0}^m (u_k^{(2)} a_{m-k,n} - (k+1)u_{k+1}b_{m-k,n} - u_k b_{m-k,n-1}), \\ b_{m,n+1} &= \frac{1}{n+1} \left(b_{m,n-2} - b_{m-1,n} \right. \\ &\quad \left. + \sum_{k=0}^m (-u_k^{(2)} b_{m-k,n} + (k+1)u_{k+1}a_{m-k,n} - u_k a_{m-k,n-1}) \right), \end{aligned} \tag{4.12}$$

$n \geq 0$, allowing one to determine $a_{0,n}$, $b_{0,n}$, $n \geq 0$ upon the knowledge of $a_{0,0}$, $b_{0,0}$. We integrate along $\pm y$ with an extrapolation step size of $\frac{1}{8}$. From (3.36) one

obtains the recursions

$$\begin{aligned} a_{m+1,n} &= \frac{1}{m+1} \sum_{k=0}^m u_k b_{m-k,n} \\ b_{m+1,n} &= \frac{1}{m+1} \left(-b_{m,n-1} + \sum_{k=0}^m u_k a_{m-k,n} \right). \end{aligned} \quad (4.13)$$

The expansion coefficients $g_{m,n}$ of $g(s, y)$ at (s_0, y_0) , are determined from (3.39) as

$$g_{m,n} = (n+1) (a_{m,n}^- a_{m,n+1} - b_{m,n}^- b_{m,n+1}) \quad (4.14)$$

where $a_{m,n}^-$, $b_{m,n}^-$ are the corresponding expansion coefficients of a and b at $(s_0, -y_0)$.

To finally determine $g(y)$ and its derivatives we write

$$\begin{aligned} g^{(n)}(y_0) &= \frac{d^n}{dy_0^n} \sum_{s_0 \in \mathbb{Z}} \int_{s_0}^{s_0+1} (s - y_0^2)^2 \frac{d^2}{ds^2} (g(s, y_0) F_{\text{GUE}}(s)) ds \\ &= \sum_{s_0 \in \mathbb{Z}} n! \sum_{m \geq 1} c_{m,n}. \end{aligned} \quad (4.15)$$

$c_{m,n}$ are the expansion coefficients of $(s, y) \mapsto \int_{s_0}^s (r - y^2)^2 \frac{d^2}{dr^2} (g(r, y) F_{\text{GUE}}(r)) dr$ at (s_0, y_0) ,

$$c_{m,n} = (m-2)(gF)_{m-1,n} - 2m(gF)_{m,n-2} + \frac{m(m+1)}{m-1}(gF)_{m+1,n-4}. \quad (4.16)$$

Here

$$(gF)_{m,n} = \sum_{k=0}^m F_k g_{m-k,n} \quad (4.17)$$

are the expansion coefficients of $g(s, y) F_{\text{GUE}}(s)$ and $F_n = -\sum_{k=1}^n \frac{k}{n} V_k F_{n-k}$ are the expansion coefficients of F_{GUE} . Numerically the sum over s_0 in (4.15) is truncated to values inside $[-15, 200]$, since outside contributions turn out to be negligible at the chosen precision goal. After accomplishing this program we keep values for $g(y)$ at $y \in \frac{1}{128}\mathbb{Z} \cap [-9, 9]$ and for $g^{(n)}(y)$, $n = 0, \dots, 4$, at $y \in \frac{1}{8}\mathbb{Z} \cap [-9, 9]$ with an accuracy of about 100 digits (a table in ASCII format is available online at [28]). For interpolating these values we deliberately used the **Interpolation**-function of the Mathematica[®] package yielding best results due to the high precision data with an interpolation order of 57.

5 Discussion of the scaling function

There have been numerous attempts to approximately determine $g(\cdot)$ [4, 29, 30, 8, 31]. For historical reasons a different scaling function, $F(\cdot)$, is analyzed in some

of these works. The relation to our scaling function $g(\cdot)$ is

$$F(\xi) = (\xi/2)^{2/3} g((2\xi^2)^{-1/3}), \quad \text{resp.} \quad g(y) = 2y F(1/(2^{1/2}y^{3/2})). \quad (5.18)$$

Note that by (1.6) the large y behavior of g is fixed by definition as $g(y) \sim 2|y|$. The special value $g(0) = 1.1503944782594709729961$ is the Baik-Rains constant [12, 6]. In the literature the universal amplitude ratio $R_G = 2^{-2/3}g(0) = 0.7247031092$ and the universal coupling constant $g^* = g(0)^{-3/2} = 0.810456700$ have been investigated. Approximate values have been determined by means of Monte-Carlo simulations for the single step model [30], numerically within a mode-coupling approximation [29, 8, 1], and even experimentally for slowly combusting paper [32] yielding estimates for $g(0)$ within reasonable ranges around the (numerically) exact value indicated.

In Figure 2 the scaling function $f(y) = \frac{1}{4}g''(y)$ is shown as determined by the

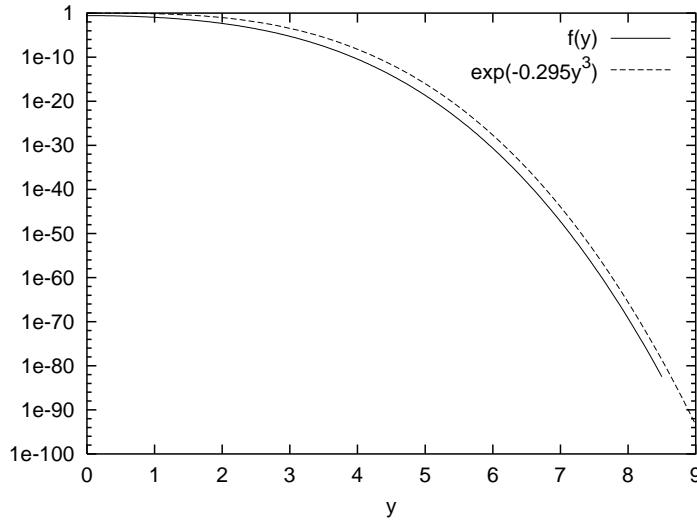


Figure 2: *The scaling function $f(y)$ versus y in a semilogarithmic plot. The dotted line $\exp(-0.295|y|^3)$ is drawn as a guide to the eye for the large y asymptotics of f .*

multiprecision expansion method explained in the previous section. We estimate its large y asymptotics as

$$\log f(y) \approx -c|y|^3 + o(|y|) \text{ for } y \rightarrow \infty. \quad (5.19)$$

The cubic behavior is very robust and numerical fits yield about 2.996–2.998 quite independently of the assumed nature of the finite size corrections. The prefactor $c = 0.295(5)$ has a relatively high uncertainty because of the unknown subleading corrections. Even though inaccessible in nature we estimate the error term, as indicated in (5.19), to be sublinear or even only logarithmic from the numerical

data. Possibly, the exact asymptotic behavior could be extracted from a refined asymptotic analysis of the Riemann-Hilbert problem.

Colaioni and Moore [1, 33] tackled the same scaling function by completely different means. Starting from the continuum version of the KPZ equation they numerically solved the corresponding mode-coupling equation [4, 8], which contains an uncontrolled approximation, since diagrams which would renormalize the three-point vertex coupling are neglected. Nevertheless a qualitative comparison of their result with the exact scaling function $f(y)$ shows reasonable similarity, cf. Figure 3. Both functions are normalized to integral 1 by definition. The mode coupling solution oscillates around 0 for $|y| > 3$, whereas $f(y) > 0$ for the exact

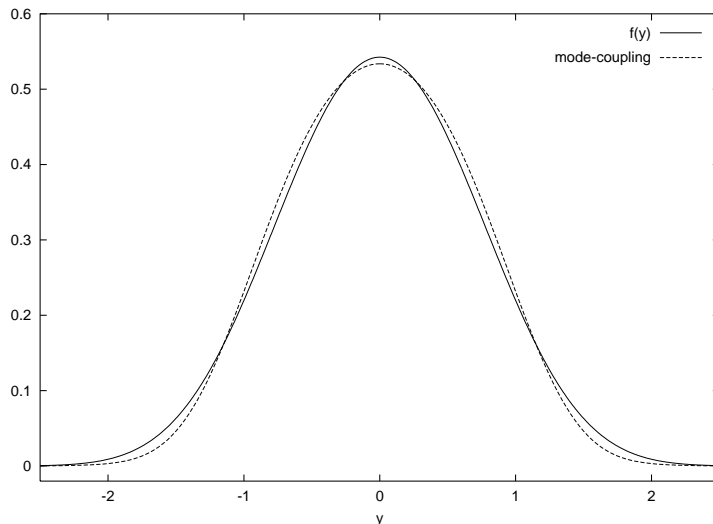


Figure 3: *The exact scaling function $f(y)$ compared to the mode coupling result of Colaioni and Moore [1](dotted line). Both functions are even.*

solution. We do not know whether this is a numerical artifact or an inherent property of the mode-coupling equation. On the other hand, the second moments are reasonably close together, 0.510523 for $f(y)$, and 0.4638 for the mode-coupling approximation. So is the value of the Baik-Rains constant $g(0) = 2 \int |y|f(y)dy$ for which mode-coupling predicts the value 1.1137.

From the solution to the mode-coupling equations one does not directly obtain $f(y)$, but rather its Fourier transform. The function $G(\tau)$ from [1] is defined through

$$G(k^{3/2}/2^{7/2}) = \hat{f}(k) = 2 \int_0^\infty \cos(ky)f(y)dy. \quad (5.20)$$

Moore and Colaioni predict a stretched exponential decay of $G(\tau)$ as $\propto \exp(-c|\tau|^{2/3})$ [33] and numerically find a superimposed oscillatory behavior on the scale $|\tau|^{2/3}$ [1]. In Figure 4 $\hat{f}(k)$ is plotted as obtained by a numerical Fourier transform of $f(y)$. Indeed it exhibits an oscillatory behavior as can be seen in Figure 5 where

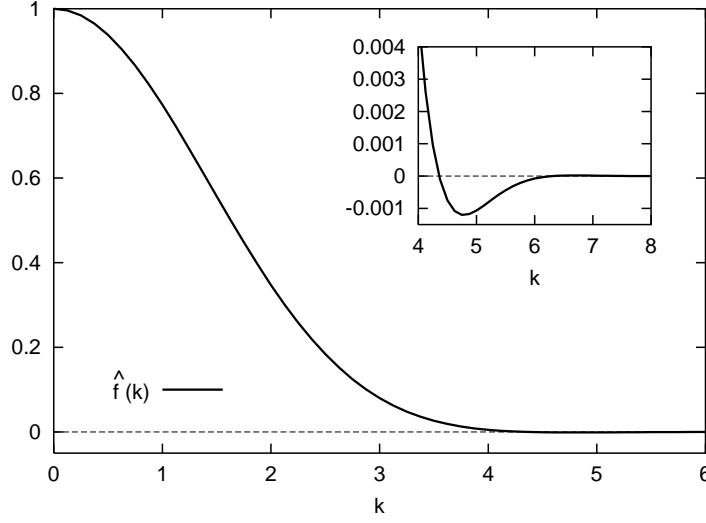


Figure 4: The Fourier transform $\hat{f}(k)$ of the scaling function $f(y)$.

the modulus of $\hat{f}(k)$ is shown on a semilogarithmic scale. The dotted line in the plot is the modulus of the function

$$10.9k^{-9/4} \sin(\frac{1}{2}k^{3/2} - 1.937)e^{-\frac{1}{2}k^{3/2}}, \quad (5.21)$$

shifted by a factor of 1000 for visibility, which fits $\hat{f}(k)$ very well in phase and amplitude for $k \gtrsim 15$. This behavior is not in accordance with the results of Colaioni and Moore, since the oscillations and the exponential decay of $G(\tau)$ for the exact solution are apparently on the scale τ and not $\tau^{2/3}$.

Note that $\hat{f}(k)$ is the scaling function for the intermediate structure function

$$S(k, t) = \int dx e^{ikx} S(x, t) \simeq 2\hat{f}(t^{2/3}k). \quad (5.22)$$

By Fourier transforming with respect to t we determine the dynamical structure function,

$$S(k, \omega) = \int dx dt e^{i(kx + \omega t)} S(x, t) \simeq 2k^{-3/2} \mathring{f}(\omega/k^{3/2}), \quad (5.23)$$

where

$$\mathring{f}(\tau) = \int ds e^{i\tau s} \hat{f}(s^{2/3}) = 2 \int_0^\infty dy \tau^{-1} L'(y/\tau^{2/3}) f(y) \quad (5.24)$$

and L has the convenient representation

$$L(\kappa) = 2 \cdot 3^{2/3} \text{Ai}(-3^{-4/3} \kappa^2) \sin(2\kappa^3/27). \quad (5.25)$$

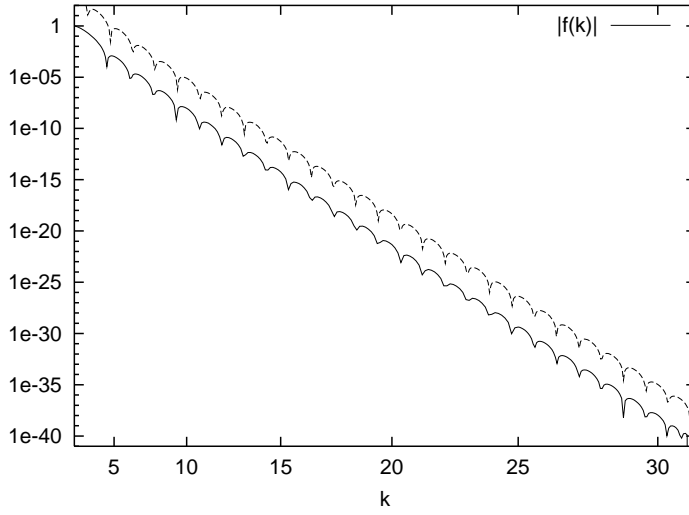


Figure 5: The modulus of $\widehat{f}(k)$ on a semilogarithmic scale. The dotted line is a heuristic fit, shifted by a factor 1000 for visibility.

The correlation function (2.6) in Fourier space is given by

$$C(k, \omega) = 2k^{-2}S(k, \omega) \sim C^{\text{KPZ}}(k, \omega) \stackrel{\text{def}}{=} 4k^{-7/2} \overset{\circ}{f}(\omega/k^{3/2}), \quad (5.26)$$

describing the asymptotic behavior at $k, \omega = 0$. Note that $C(k, \omega) > 0$ by definition, since $\langle h_{k,\omega} h_{k',\omega'} \rangle = \delta_{k,-k'} \delta_{\omega,-\omega'} C(k, \omega)$ for $(k, \omega) \neq (0, 0)$. The anomalous scaling behavior in real space is reflected by the exponents for the divergence of $C^{\text{KPZ}}(k, \omega)$ at $k = \omega = 0$. In the linear case, the Edwards-Wilkinson equation $\lambda = 0$ in (1.1), one easily obtains

$$C^{\text{EW}}(k, \omega) = \frac{D}{\omega^2 + \nu^2 k^4}. \quad (5.27)$$

A 3d-plot of $C^{\text{KPZ}}(k, \omega)$ is shown in Figure 6. Its striking features are the smooth behavior away from $k, \omega = 0$, especially on the lines where $k = 0$ and $\omega = 0$ and the two symmetric maxima of $k \mapsto C^{\text{KPZ}}(k, \omega)$ for constant ω . Our numerical data yield for the singular behavior at $k = 0, \omega = 0$,

$$\begin{aligned} C^{\text{KPZ}}(k, \omega) &= \omega^{-7/3} (2.10565(1) + 0.85(1) k^2 \omega^{-4/3} + \mathcal{O}(k^4 \omega^{-8/3})), \\ &= k^{-7/2} (19.4443(1) - 52.5281(1) \omega^2 k^{-3} + \mathcal{O}(\omega^4 k^{-6})). \end{aligned} \quad (5.28)$$

6 Conclusions and Outlook

For systems close to equilibrium many properties valid in generality rely on detailed balance, amongst them in particular the link between correlation and response functions. The KPZ equation does not satisfy detailed balance, since the

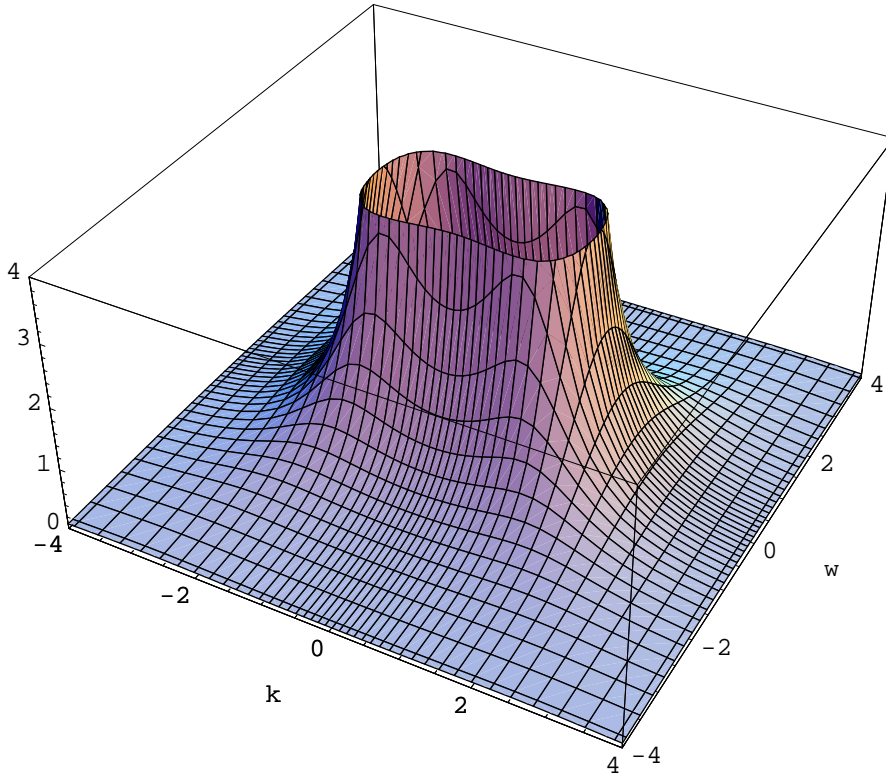


Figure 6: *The correlation function $C(k, \omega)$ in Fourier space.*

growth is directed. However, it has been speculated that in $1+1$ dimensions detailed balance is recovered in the scaling regime. With our exact scaling function at hand, such a claim can be tested.

Detailed balance implies that the eigenvalues of the generator in the master equation lie on the negative real axis. Thus autocorrelations in the form $\langle X(t)X(0) \rangle$ can be written as the Laplace transform of a positive measure. The structure function $S(k, t)$ at fixed k is such an autocorrelation. Using the scaling form (5.22) detailed balance would imply

$$S(k, t) = \int_{-\infty}^0 \nu(|k|^{-3/2} d\lambda) e^{\lambda|t|} \quad (6.1)$$

with $\nu(d\lambda) \geq 0$. In particular $S(k, t) \geq 0$. From (5.21) we know that $S(k, t)$ oscillates around zero. Definitely, at $|k| \approx 5$ there is a negative dip, cf. Fig. 4. Thus (6.1) cannot be correct.

The Bethe ansatz [34, 35] indicates that, for large system size, the density of states is concentrated on an arc touching 0. If so, the integration in (6.1) would have to be replaced by a corresponding line integral. It is not clear to us how to extract from the numerical knowledge of $S(k, t)$ such a representation.

Our main result is the exact scaling function f , see Figure 3, for the two-point

function of the stationary KPZ equation in $1 + 1$ dimensions. “Exact” must be qualified in two respects. Firstly f is given indirectly through the solution of certain differential equations, which can be solved numerically only with considerable effort. The errors are well controlled, however. Secondly, we rely on universality, in the sense that the scaling function is derived for the PNG model, which is one rather particular model within the KPZ universality class. Of course, it would be most welcome to establish the scaling limit also for other models in this class.

The KPZ equation (1.1) is a two-dimensional field theory and, in spirit, belongs to the same family as two-dimensional models of equilibrium statistical mechanics, one-dimensional quantum spin chains, and other $(1 + 1)$ -dimensional quantum field theories at zero temperature. While in the latter cases, there are a number of models for which the two-point function can be computed, in the dynamical context such solutions are scarce. In addition, the KPZ equation does not satisfy the condition of detailed balance. Such nonreversible models are known to be difficult and we believe that the PNG model is the first one in the list of exact solutions, disregarding noninteracting field theories.

For the nonstationary KPZ equation with a macroscopic profile of nonzero curvature the analogue of F_0 is the Tracy-Widom distribution function. In that case the full statistics of $x \mapsto h(x, t)$ for large but fixed t is available [7]. It is conceivable that an extension of the techniques used there also admits a more detailed study of, say, the joint distribution of $h(x, t) - h(0, 0)$, $h(x', t) - h(0, 0)$. On the other hand the joint distribution of $h(0, t) - h(0, 0)$, $h(0, t') - h(0, 0)$ does not seem to be accessible. In the representation through the directed polymers it means that space-like points, even several of them, can be handled, whereas time-like points remain a challenge.

Acknowledgements. We greatly enjoyed the collaboration with Jinho Baik at the early stage of this project and are most grateful for his important input. We also thank Mike Moore for providing us with the numerical solution of the mode-coupling equation.

References

- [1] Francesca Colaiori and M. A. Moore. Numerical solution of the mode-coupling equations for the Kardar-Parisi-Zhang equation in one dimension. *Phys. Rev. E*, 65:017105, 2002.
- [2] M. Kardar, G. Parisi, and Y. Z. Zhang. Dynamic scaling of growing interfaces. *Phys. Rev. Lett.*, 56:889–892, 1986.
- [3] D. Forster, D. R. Nelson, and M. J. Stephen. Large-distance and long-time properties of a randomly stirred fluid. *Phys. Rev. A*, 16:732–749, 1977.

- [4] H. van Beijeren, R. Kutner, and H. Spohn. Excess noise for driven diffusive systems. *Phys. Rev. Lett.*, 54(18):2026–2029, 1985.
- [5] Michael Prähofer and Herbert Spohn. Current fluctuations for the totally asymmetric simple exclusion process. In Sidoravicius Vladas, editor, *In and out of equilibrium*, volume 51 of *Progress in Probability*, pages 185–204. Birkhauser Boston, 2002.
- [6] Michael Prähofer and Herbert Spohn. Universal distributions for growth processes in one dimension and random matrices. *Phys. Rev. Lett.*, 84(21):4882–4885, 2000.
- [7] Michael Prähofer and Herbert Spohn. Scale invariance of the PNG droplet and the Airy process. *J. Stat. Phys.*, 108(5–6):1071–1106, 2002.
- [8] Erwin Frey, Uwe Claus Täuber, and Terence Hwa. Mode-coupling and renormalization group results for the noisy Burgers equation. *Phys. Rev. E*, 53(5):4424–4438, 1996.
- [9] T.T. Wu, B.M. McCoy, C.A. Tracy, and E. Barouch. The spin-spin correlation function of the 2-dimensional Ising model: exact results in the scaling region. *Phys. Rev. B*, 13:316, 1976.
- [10] Thomas Spencer. A mathematical approach to universality in two dimensions. *Physica A*, 279(1-4):250–259, 2000.
- [11] Craig A. Tracy and Harald Widom. Level spacing distribution and the Airy kernel. *Commun. Math. Phys.*, 159:151–174, 1994.
- [12] Jinho Baik and Eric M. Rains. Limiting distributions for a polynuclear growth model with external sources. *J. Stat. Phys.*, 100(3-4):523–541, 2000.
- [13] Jinho Baik. Riemann–Hilbert problems for last passage percolation. *math.PR/0107079*, 2001.
- [14] Vipul Periwal and Danny Shevitz. Unitary-matrix models as exactly solvable string theories. *Phys. Rev. Lett.*, 64(12):1326–1329, 1990.
- [15] Timo Seppäläinen. A microscopic model for the Burgers equation and longest increasing subsequences. *Electronic J. Prob.*, 1(5):1–51, 1996.
- [16] Gabor Szegő. *Orthogonal Polynomials*. American Mathematical Society Providence, Rhode Island, 1967.
- [17] M. Hisakado. Unitary matrix models and Painlevé III. *Mod. Phys. Letts A*, 11:3001–3010, 1996.

- [18] Craig A. Tracy and Harald Widom. Random unitary matrices, permutations and Painlevé. *Commun. Math. Phys.*, 207(3):665–685, 1999.
- [19] Alexei Borodin. Discrete gap probabilities and discrete Painlevé equations. *math-ph/0111008*, 2001.
- [20] S. P. Hastings and J. B. McLeod. A boundary value problem associated with the second Painlevé transcendent and the Korteweg-de Vries equation. *Arch. Rat. Mech. Anal.*, 73:31–51, 1980.
- [21] Jinho Baik, Persi Deift, and Kurt Johansson. On the distribution of the length of the longest increasing subsequence of random permutations. *J. Amer. Math. Soc.*, 12:1119, 1999.
- [22] Michael Prähofer and Herbert Spohn. Statistical self-similarity of one-dimensional growth processes. *Physica A*, 279(1-4):342–352, 2000.
- [23] Jinho Baik and Eric M. Rains. Algebraic aspects of increasing subsequences. *Duke Math. J.*, 109(1):1–65, 2001.
- [24] Craig A. Tracy and Harald Widom. private communication. 1999.
- [25] Milton Abramowitz and Irene A. Stegun, editors. *Pocketbook of Mathematical Functions*. Verlag Harri Deutsch, Thun - Frankfurt am Main, 1984.
- [26] David Barton, I. M. Willers, and R. V. M. Zahar. Taylor series methods for ordinary differential equations – An evaluation. In John Rice, editor, *Mathematical Software*, pages 369–390. Academic Press, New York, 1971.
- [27] Siddharta Chatterjee. MPFUN++, a C++-based multiprecision system. <http://www.cs.unc.edu/Research/HARPOON/mpfun++/>, 2000.
- [28] Michael Prähofer and Herbert Spohn. The scaling function $g(y)$. <http://www-m5.ma.tum.de/KPZ/>, 2002.
- [29] Terence Hwa and Erwin Frey. Exact scaling function of interface growth dynamics. *Phys. Rev. A*, 44:R7873–R7876, 1991.
- [30] Lei-Han Tang. Steady-state scaling function of the (1+1)-dimensional single-step model. *J. Stat. Phys.*, 67:819–826, 1992.
- [31] Hans C. Fogedby. Scaling function for the noisy Burgers equation in the soliton approximation. *Europhys. Lett.*, 56(4):492–498, 2001.
- [32] M. Myllys, J. Maunuksela, M. Alava, J. Merikoski, and J. Timonen. Kinetic roughening in slow combustion of paper. *Phys. Rev. E*, 64(036101):1–12, 2001.

- [33] Francesca Colaioni and M. A. Moore. Stretched exponential relaxation in the mode-coupling theory for the Kardar-Parisi-Zhang equation. *Phys. Rev. E*, 63:057103, 2001.
- [34] Leh-Hun Gwa and Herbert Spohn. Six-vertex model, roughened surfaces, and an asymmetric spin Hamiltonian. *Phys. Rev. Lett*, 68:725–728, 1992.
- [35] Leh-Hun Gwa and Herbert Spohn. Bethe solution for the dynamical-scaling exponent of the noisy Burgers equation. *Phys. Rev. A*, 46:844–854, 1992.